Effect of Sol−Gel Confinement on the Structural Dynamics of the Enzyme Bovine Cu,Zn Superoxide Dismutase

Isabel Pastor,[†] Manuel Prieto,[‡] and C. Reyes Mateo*[,†]

Instituto de Biología Molecular y Celular, Universidad Miguel Hernández, 03202-Elche, Spain, and Centro de Química-Física Molecular and IN- Institute of Nanosciences and Nanotechnology, Instituto Superior Técnico, Av. Rovisco Pais, P-1049-001, Lisboa, Portugal

Received: June 18, 2008; Revised Manuscript Received: September 3, 2008

Immobilization of proteins in sol−gel glasses has allowed the development of a new generation of robust and sensitive analytical devices as well as contributes to the investigation of the effect of molecular confinement on the structure of proteins. The immobilized protein usually preserves its structural integrity and functionality, while interactions with the matrix and its surface seem to contribute to alter its dynamics and stability. With the aim of better understanding the nature of such interactions, we have encapsulated the enzyme bovine Cu,Zn superoxide dismutase (BSOD), negatively charged at physiological pH, in a sol−gel matrix and the photophysical properties of its single tyrosine have been determined using both steady-state and time-resolved fluorescence techniques. Fluorescence spectra, quenching experiments, fluorescence lifetimes, and anisotropy measurements indicate that immobilization does not lead to any major conformational change, at least in the region of protein where the tyrosine residue is located. In addition, fluorescence anisotropy decays recorded above and below the isoelectric point of the protein indicate that, at neutral pH, well above its isoelectric point, the entrapped BSOD freely rotates within the matrix pore, but showing a different rotational behavior as compared with that in the bulk aqueous solution. However, below the isoelectric point, the global motion of the protein is totally hindered upon entrapment. Electrostatic interactions with the gel matrix, changes in water viscosity, and protein-to-pore size ratio are discussed as possible factors responsible for this behavior.

Introduction

Understanding the physical changes that a protein can undergo upon adsorption or encapsulation in a solid support is fundamental to the development and application of modern protein technology.[1,2] Encapsulation further provides a platform for examining the influence of confinement on protein stability, that can serve as a model of the crowded in vivo cellular environment.[3−7] An emerging technique for immobilization involves the entrapment of a protein into porous inorganic silicate matrixes formed by a low temperature sol−gel processing method.[8−11] Following a reaction of hydrolysis and polycondensation of alkosides, the proteins are individually caged and retained in pores varying from 20 to 100 Å in diameter, being accessible to small molecules diffusing into the matrix, all of which enable applications in biosensors and biotechnology.[12,13] The entrapped protein vicinity is completely different from the native environment. The biomolecule usually preserves its structural integrity and functionality, while excluded volume effects, the perturbation of water structure, and noncovalent interactions with the gel matrix all seem to contribute to alter its dynamics and stability.

In order to get more insight into the nature of the protein−matrix interactions and how they might be modulated in a rational way, we recently encapsulated in a sol−gel matrix the model protein lysozyme, which is highly positively charged at neutral pH (isoelectric point ∼11), and its dynamical behavior at different ionic strength and pH was analyzed (always below its isoelectric point, since the sol−gel matrix is not stable in alkaline media).[14] Results demonstrated, for the first time, the existence of strong electrostatic interactions between the protein molecule and the negatively charged sol−gel walls (with an isoelectric point of ∼2) which were, ultimately, responsible for the total arrest of the overall rotation of the protein. Our results were consistent with the significantly restricted rotation observed, at neutral pH, for myoglobin (pI ∼ 7.2)[15] and for highly basic horse heart cytochrome *c* (pI 9.45),[16] and with those reported for the green fluorescent protein mutant GFPmut2[17] and the highly acidic Fe^{3+} cytochrome b_5,[16] both negatively charged at physiological pH. These last works showed that the protein environment inside the silica pores is similar or slightly more viscous than the one sensed by the protein in the aqueous solution, and that unhindered molecular rotations occur. On the contrary, for the human serum albumin[18] and for the alkaline phosphatase,[19] significant restriction of its global rotational motion has been observed in spite of its overall negative charge at physiological pH, suggesting that other factors, besides electrostatic interactions, contribute to alter the dynamics of the entrapped protein.

With the aim of better clarifying the role of putative protein−matrix interactions on the structural and dynamic properties of sol−gel entrapped biomolecules, we have encapsulated the enzyme bovine Cu,Zn superoxide dismutase (BSOD), which is negatively charged at physiological pH (pI 4.95), and therefore likely to be repelled at neutral pH by the silica surface of the sol−gel matrix. The protein was selected, since at, difference of lysozyme, it was possible to work at pH values below and above its pI, drastically changing its electric charge and, therefore, the nature of its interaction with the sol−gel matrix. BSOD is a dimeric enzyme of molecular mass 32 000 Da, which catalyzes the dismutation of the superoxide free

* Corresponding author. Fax: +34 966 658 758. E-mail: rmateo@umh.es.
[†] Universidad Miguel Hernández.
[‡] Instituto Superior Técnico.

10.1021/jp805368s CCC: $40.75
Published on Web 11/01/2008

radical to oxygen and hydrogen peroxide, participating in the cellular defense mechanism against oxidative damage.[20,21] This protein has been previously immobilized in a sol−gel matrix with analytical applications, to build optical and electrochemical biosensors;[22−24] however, an exhaustive characterization of its biophysical properties upon encapsulation has not been carried out to date. BSOD contains a single tyrosine residue (Tyr-108) per subunit, which is fluorescent and solvent exposed, and no tryptophan residue.[25] In the present work, BSOD was entrapped in sol−gel matrices prepared from tetraethyl orthosilicate through an alcohol-free sol−gel route, and the photophysical properties of its fluorescent tyrosine were characterized in detail. Results suggest that immobilization does not lead to any major conformational change, at least in the region of protein where the Tyr-108 residue is located. Time-resolved anisotropy decays, recorded at pH 7.4 and 3.5, indicate that the internal dynamics of BSOD is preserved upon immobilization, although the protein shows a different rotational behavior as compared with that in the bulk aqueous solution, especially when the pH is kept below its isoelectric point.

Materials and Methods

Chemicals. Bovine erythrocyte copper−zinc superoxide dismutase (BSOD) (E.C.1.15.1.1, 2610 U mg^{-1}), tetraethyl orthosilicate (TEOS), and *N*-acetyl-L-tyrosine amide (NATyrA) were purchased from Sigma−Aldrich Chemical (Milwauke, WI) and were used without further purification. All other chemicals were of analytical or spectroscopic reagent grade. Sodium phosphate buffers (10 mM, pH 7.4) were prepared with deionized doubly distilled water. The BSOD concentration was determined from UV absorbance at 278 nm, using an extinction coefficient of $\varepsilon = 3230\ M^{-1}\ cm^{-1}$.[26]

Immobilization of BSOD in Sol−Gel Monoliths. BSOD was encapsulated in pure silica matrices through the alcohol free sol−gel route described in Ferrer et al.[27] (2002). Briefly, 4.46 mL of TEOS, 1.44 mL of H_2O, and 0.04 mL of HCl (0.62 M) were mixed under vigorous stirring at 22 °C in a closed vessel. After 1 h, 1 mL of the resulting sol was mixed with 1 mL of deionized water and submitted to rotaevaporation for a weight loss of 0.62 g (i.e., 0.62 g is approximately the alcohol mass resulting from alkoxyde hydrolysis). A 300 μL portion of the aqueous sol was mixed with 300 μL of buffered BSOD (300 μM) in a disposable cuvette of polymethylmethacrylate. Gelation occurs readily after mixing. Following gelation, monoliths were wet aged in the phosphate buffer solution at 4 °C for 48 h. After aging, the monoliths, having a size of ~4 mm × 4 mm × 19 mm, were removed from the disposable cuvettes and placed in 5 mm^2 quartz cuvettes in the presence of 250 μL of desired buffer. In most experiments, this buffer was sodium phosphate buffer 10 mM, pH 7.4 (higher phosphate concentrations were avoided to prevent tyrosine−phosphate interactions). For quenching experiments, the same buffer containing acrylamide was used, while, for acid pH experiments, it was replaced by citrate-phosphate buffer pH 3.5, and these were allowed to equilibrate for 48 h before being measured. Blank monoliths were prepared as above but by replacing the protein solution by the working buffer.

Absorption and Steady-State Fluorescence Measurements. Absorption measurements were carried out at room temperature using a Shimadzu spectrophotometer (UV-1603, Tokio, Japan). Fluorescence spectra, quenching measurements, and steady-state anisotropy, $\langle r \rangle$, were performed with a SLM-8000C spectrofluorimeter (SLM Instruments Inc., Urbana, IL) fitted with Glan-Thompson polarizers. The experimental samples (sol−gel monoliths and protein aqueous solution) were placed in 5 mm × 5 mm path length cuvettes. For quenching and steady-state anisotropy measurements, samples were excited at 285 nm and emission was detected at 320 nm. Background intensities due to the sol−gel matrix were always taken into account and subtracted from the sample.

Time-Resolved Fluorescence Measurements. The decay of the total fluorescence intensity, and those of the parallel and perpendicular components, were recorded at 22, 30, and 40 °C in a single-photon timing system as previously described.[28] The experimental samples (sol−gel monoliths and protein aqueous solution) were placed in 5 mm × 5 mm path length cuvettes and excited at 285 nm through a frequency doubled, cavity dumped (3.7 MHz repetition rate), dye laser of rhodamine 6G (Coherent 701-2), synchronously pumped by a mode-locked Ar^+ laser (514.5 nm, Coherent Innova 400-10). The emission was detected by a Hamamatsu R-2809 MCP photomultiplier at 320 nm (Jobin-Yvon HR320 monochromator). The instrumental response function (80 ps) was generated from a scatter dispersion (silica, colloidal water solution). The time scaling was 8.4 ps per channel, and 1024 channels were in use. A minimum of 20 000 counts were recorded in the top channel for the decay of the total intensity and that for the parallel component, while ~15 000 counts were recorded for the perpendicular component. Integrated areas under these decay curves were approximately 3.7×10^6, 2.7×10^6, and 2.0×10^6, respectively.

The kinetic parameters of the impulse response fluorescence intensity decay, $i(t)$ (lifetimes, τ_i, and normalized amplitudes, α_i), were determined by reconvolution and fitting, using nonlinear least-squares regression methods. The amplitude-weighted lifetime proportional to quantum yield, $\bar{\tau}$, and the average fluorescence lifetime, $\langle \tau \rangle$, were calculated according to[29] $\bar{\tau} = \sum \alpha_i \tau_i$ and $\langle \tau \rangle = \sum_i \alpha_i \tau_i^2 / \sum_i \alpha_i \tau_i$, respectively. The anisotropy decay function, $r(t)$, was determined using a nonlinear least-squares global analysis method by simultaneously fitting the vertically and horizontally polarized emission components to a sum of n exponentials and a constant term:[30]

$$r(t) = (r(0) - r_\infty)[\sum_{i=1}^{n} \beta_i \exp(-t/\varphi_i)] + r_\infty \qquad (1)$$

where φ_i are the rotational correlation times, β_i are normalized amplitudes, and r_∞ is the residual anisotropy, containing information about the restriction of the depolarizing processes. To perform this analysis, the first channels of the experimental decays were not included in the fit, in order to avoid different scattering contributions from the sol−gel monolith among different samples.

The fit tabulated here both for fluorescence intensity and for anisotropy decay represents the minimum set of adjustable parameters which satisfy the usual statistical criteria, namely, a reduced χ^2 value of <1.3 and a random distribution of weighted residuals.

Quenching Experiments. The accessibility to solvent and the ionic environment of the fluorescent tyrosine in the free and sol−gel entrapped BSOD were analyzed by monitoring the fluorescence quenching induced by adding increasing amounts of stock solutions of neutral (acrylamide) or charged quenchers, I^- (as KI) to the protein sample (150 μM). To prevent iodide oxidation, $Na_2S_2O_3$, at a final concentration of 200 μM, was added to the KI solution. For the quenching studies of the entrapped protein, the diffusion constraints imposed by the dimensions of the monoliths and the restriction to the free

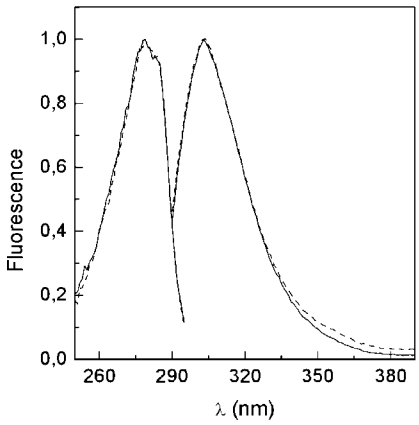

Figure 1. Normalized excitation (λ_{em} = 320 nm) and emission (λ_{ex} = 285 nm) spectra of 150 μM BSOD in buffer (—) and entrapped in a sol−gel matrix (- - -).

diffusion of the quencher through the sol−gel matrix required its incubation with the quencher solution for at least 48 h before concentration gradients could be neglected. A different monolith containing the same protein concentration was incubated with each quenching concentration. Data were analyzed by Stern−Volmers plots of I_0/I versus $[Q]$,[31] where I_0 and I stand for the steady-state fluorescence intensities in the absence and in the presence of quencher, respectively, and $[Q]$ is the quencher concentration. Since these plots were linear, the "static" quenching contribution was considered <10% and the Stern−Volmer constant, K_{SV}, was directly obtained from the slope of the line.[31] This parameter was used to calculate the bimolecular rate constant of the quenching process, k_Q, from the expression $K_{SV} = k_Q\langle\tau\rangle$.[32] *N*-Acetyl-L-tyrosine amide (NATyrA) was taken as a control for a fully accessible residue.

Results and Discussion

Effect of Sol−Gel on the Photophysical Properties of BSOD. Normalized fluorescence excitation and emission spectra of BSOD in buffer and entrapped in sol−gel matrices are shown in Figure 1. The spectra show the characteristic bands for tyrosine and were almost identical for both systems, indicating that BSOD was successfully encapsulated in sol−gel glass and that Tyr-108 is located in a very similar microenvironment upon sol−gel encapsulation.[33] There is no indication of broadening of the emission peak in the entrapped protein (a width at half-maximum of about 30−35 nm as with L-tyrosine), which suggests that Tyr-108 residue is not involved in hydrogen-bonded complexes with the silanol groups of the silica matrix, negatively charged at physiological pH.

Further information regarding the environment of the fluorescent tyrosine was obtained from the analysis of decay of the fluorescence emission of the free and entrapped BSOD, recovered at three temperatures. Experimental decays were best fitted to triexponential functions. This triexponential behavior has been similarly reported for other proteins and peptides with a single tyrosine residue,[34−37] and reflects the existence of ground-state rotamers sensing different chemical environments.[38,39] Fluorescence fit parameters, including $\bar{\tau}$ and $\langle\tau\rangle$, are shown in Table 1 as well as the fluorescence quantum yield of the protein, which was estimated from $\bar{\tau}$ and the radiative lifetime of tyrosine (27 ± 2 ns).[33,40] Quantum yield and average lifetimes are found to be very similar at the three temperatures, for the protein either in buffer solution or encapsulated in the sol−gel matrix, but the lifetimes (τ_i) and their relative amplitudes (α_i) are affected in a different way by temperature. In solution, the amplitude α_3 tends to decrease when temperature is increased, while α_2 increases and α_1, τ_1, and τ_2 are practically nonsensitive to temperature. This systematic trend suggests that the three fluorescence exponentials recovered in solution represent three different rotameric states of Tyr-108. However, a more complex behavior is observed for the encapsulated system: the amplitudes and lifetimes do not follow a definite trend as temperature is increased. This behavior suggests that the environment surrounding Tyr-108 residue upon encapsulation is more heterogeneous than that for the free protein and that not only temperature but also other effects, such as confinement, electrostatic interactions, or changes in water viscosity, modify the number and contribution of conformations probed by Tyr-108 in BSOD, and/or the rotamer interconversion rate.[41]

Accessibility of Quenchers to Tyr-108 in the Sol−Gel Entrapped BSOD. The effect of acrylamide and iodide on the intrinsic fluorescence of the entrapped BSOD was examined and compared with that observed for the free protein and for the fully accessible NATyRA. The Stern−Volmer plots were linearly dependent on the quencher concentration, and K_{SV} was directly obtained from the slope of the line and used to calculate the bimolecular rate constant of the quenching process, k_Q (Figure 2 and Table 2). In the case of acrylamide, the k_Q value of the free protein is 3.7 ± 0.3, which is about 25% lower than the value measured for the fully accessible NATyrA under the same conditions, probably due to the difference in the diffusion coefficients of Tyr-108 relative to free NATyrA.[42] This result is consistent with a situation in which Tyr-108 is quite exposed to the solvent, in full agreement with the X-ray structure of the protein.[20] In contrast, a clear decrease is observed for the entrapped system whose k_Q value drops from 3.7 to 1.9 M^{-1} ns^{-1}. There are several possible explanations for this behavior, which include a lower rate diffusion of the quencher within the glass matrix, as compared to the aqueous solution,[43] or a reduction of the accessibility of acrylamide to Tyr-108, probably due to a conformational change in the entrapped protein, at least at the region where tyrosine is located. Experiments with iodide showed a much less efficient quenching process (Table 2). This indicates that Tyr-108 should have a net negatively charged microenvironment, probably due to the proximity of anionic residues such as Glu-107, which is maintained upon protein entrapment. We also used a positively charged quencher (Cs^+), but the results were erratic due to its low quenching efficiency (data not shown).[42]

Effect of Sol−Gel on the Dynamics Properties of BSOD. The dynamic changes induced in BSOD upon sol−gel immobilization were studied from the fluorescence anisotropy of Tyr-108. As a first step, we analyzed the effect of sol−gel encapsulation on the steady-state anisotropy, as a function of temperature and at physiological pH (Figure 3). The anisotropy values determined for the entrapped BSOD were similar to those observed in solution, through the temperature range investigated. This result does not necessarily indicate the same dynamic behavior for the free and the encapsulated protein. It should be stressed that the anisotropy values obtained under continuous illumination simultaneously contain both structural and dynamic information about the protein which cannot be discriminated from a simple steady-state experiment.[44] To make this information available, the fluorescence anisotropy decay of the protein was recorded at 22, 30, and 40 °C in solution and within the sol−gel matrix (Figure 4). The results of the deconvolution analysis of the experimental data are listed in Table 3. In solution, at least two well separated rotational correlation times

TABLE 1: Photophysical Parameters of BSOD (Fluorescence Lifetimes, τ_i, Normalized Amplitudes, α_i, Amplitude-Weighted Lifetimes, $\bar{\tau}$, Average Fluorescence Lifetimes, $\langle\tau\rangle$, and Quantum Yields, Φ) in Solution and Immobilized in Sol−Gel Matrixes under Different Experimental Conditions

medium	*T*/°C	α_1 ±0.01	τ_1 (ns) ±0.1	α_2 ±0.01	τ_2 (ns) ±0.1	α_3 ±0.01	τ_3 (ns) ±0.1	$\bar{\tau}$ (ns)	$\langle\tau\rangle$ (ns)	Φ^a	χ^2
buffer	22	0.13	0.3	0.59	1.1	0.28	2.0	1.25	1.47	0.046	1.09
pH 7.4	30	0.13	0.2	0.77	1.1	0.13	2.3	1.17	1.39	0.043	1.02
	40	0.11	0.2	0.85	1.1	0.04	2.6	1.06	1.23	0.040	1.13
sol−gel	22	0.12	0.3	0.56	1.1	0.32	2.0	1.29	1.51	0.048	1.00
pH 7.4	30	0.18	0.4	0.74	1.3	0.08	2.7	1.25	1.86	0.046	1.05
	40	0.12	0.2	0.70	1.0	0.18	2.4	1.08	1.31	0.040	1.10
sol−gel pH 3.5	30	0.09	0.3	0.59	1.1	0.32	2.0	1.32	1.52	0.049	1.14

[a] Determined from $\Phi = \bar{\tau}/\tau_r$, where $\tau_r = 27 \pm 2$ ns is the radiative lifetime of tyrosine.[33,40]

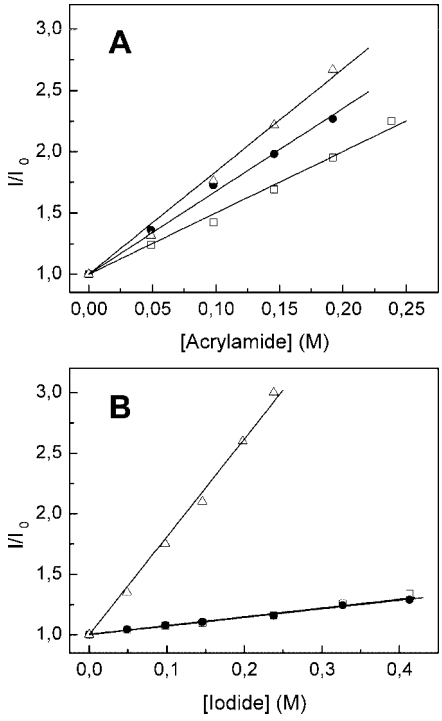

Figure 2. Stern−Volmer plots for acrylamide (A) and iodide (B) quenching of NATyrA (△) and 150 μM BSOD in solution (●) and entrapped in a sol−gel matrix (□). Samples were excited at 285 nm, and fluorescence was recorded at 320 nm.

TABLE 2: Acrylamide and Iodide Quenching Constants (K_{SV} and k_Q) of Free BSOD, Sol−Gel Entrapped SOD and NATyrA ($T = 22$°C; pH 7.4)

	BSOD (solution)	BSOD (sol−gel)	NATyrA
	Acrylamide		
K_{SV} (M^{-1})	5.4 ± 0.2	2.9 ± 0.1	8.2 ± 0.2
k_Q (M^{-1} ns^{-1})	3.7 ± 0.3	1.9 ± 0.2	5.1 ± 0.3[a]
	Iodide		
K_{SV} (M^{-1})	0.7 ± 0.1	0.8 ± 0.2	8.5 ± 0.2
k_Q (M^{-1} ns^{-1})	0.5 ± 0.3	0.5 ± 0.3	5.3 ± 0.2

[a] Determined from $k_Q = K_{SV}/\langle\tau\rangle$, considering $\langle\tau\rangle = 1.6$ ns.[41]

were needed to describe the decay processes: The fast one φ_1, around 0.2−0.3 ns, accounts for between 31 and 38% of the total depolarization. The remaining anisotropy decays completely through the slow rotational component, φ_2, whose value slightly decreases with temperature. Since $\varphi_1 \ll \varphi_2$, the decay of the total anisotropy was expressed as the product of two depolarizing processes, one due to fast restricted segmental

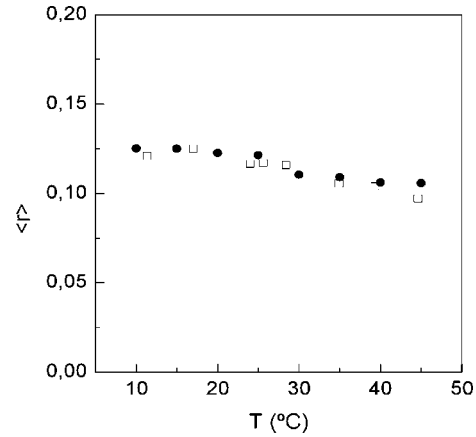

Figure 3. Variation of the steady-state fluorescence anisotropy, $\langle r\rangle$, with temperature of BSOD in solution (●) and entrapped in a sol−gel matrix (□). Samples were excited at 285 nm, and fluorescence was recorded at 320 nm.

motion of the tyrosine residue ($r'(t)$) and another related to the global rotation motion of the whole protein as[45]

$$r(t) = r'(t)\exp(-t/\varphi_{global}) \quad (2)$$

where $r'(t) = r(0)[(1 - S_1^2)\exp(-t/\varphi_{segmental}) + S_1^2]$, with S_1 being the order parameter characterizing the internal fluctuation of the peptidic segment containing the tyrosine residue. Comparing eqs 1 and 2, the long and short rotational correlation times obtained from the fit can be respectively related to φ_{global} and $\varphi_{segmental}$ by $\varphi_2 = \varphi_{global}$ and $\varphi_1 = [(1/\varphi_{segmental}) + (1/\varphi_{global})]^{-1}$ (Table 4).

The rate of the segmental motions experienced by Tyr-108 within the protein ($\varphi_{segmental}$) is found to be independent of temperature and relatively restricted, as shown from the value obtained for S_1. The average angular oscillations of these motions were estimated from S_1, assuming the "wobbling-in-cone" model.[46] For this model, the half-angle θ_0 of the cone within which the segment containing tyrosine freely rotates is given by $\cos\theta_0 = (1/2)[(8S_1 + 1)^{1/2} - 1]$. An angle of around 29° is obtained for the protein in solution at 22 °C, which is similar to that obtained by Ferreira et al. for the same protein under the same conditions,[25] and is practically preserved through the temperature range investigated (Table 4). The $r(0)$ value recovered from the fit is lower than the value expected for an immobilized tyrosine residue upon excitation to 285 nm.[34] The existence of an additional ultrafast motion on the subpicosecond/picosecond time scale that cannot be observed with our instrument is likely to be one source of this depolarization,

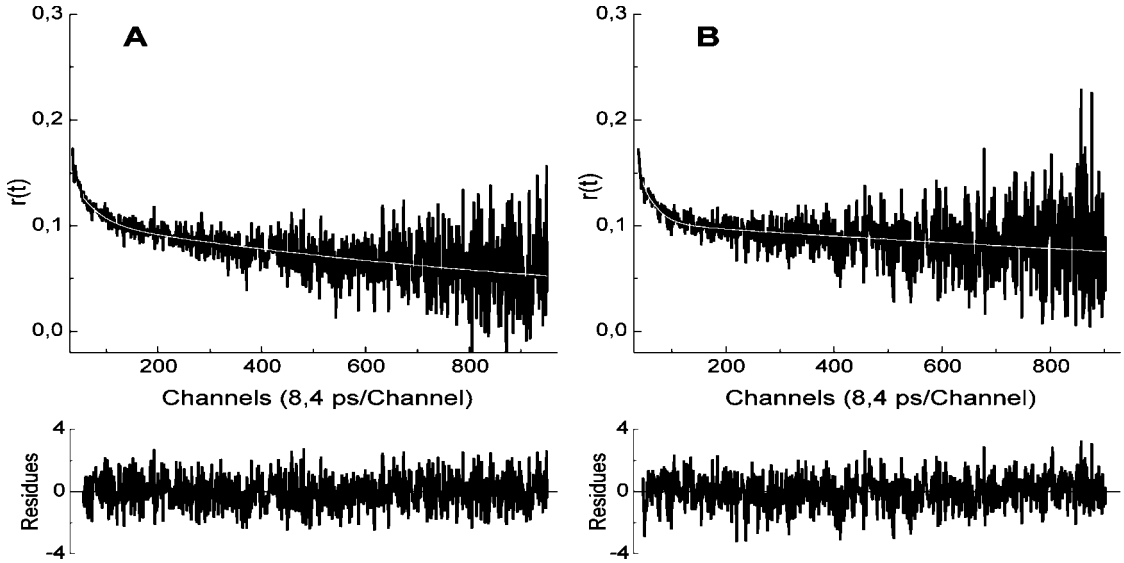

Figure 4. Time-resolved fluorescence anisotropy of BSOD in solution (A) and entrapped in a sol−gel matrix (B) at 30 °C. The decay fit obtained from eq 1 is superimposed over the collected data. Residuals of the fits are also shown.

TABLE 3: Time-Resolved Fluorescence Anisotropy Parameters of BSOD (Rotational Correlation Times, φ_i, Amplitudes, β_i, and Residual Anisotropy, r_∞) in Solution and Immobilized in Sol−Gel Matrices

medium	T (°C)	$r(0)$	β_1	φ_1 (ns)	β_2	φ_2 (ns)	r_∞	χ^2
buffer	22	0.18	0.32	0.3	0.68	12	0	1.12
pH 7.4	30	0.16	0.31	0.2	0.69	11	0	1.15
	40	0.16	0.38	0.3	0.62	9	0	1.07
sol−gel	22	0.16	0.36	0.2	0.64	23−30	0	*a*
pH 7.4	30	0.17	0.36	0.2	0.64	24−35	0	*a*
	40	0.15	0.38	0.2	0.62	23−42	0	*a*
sol−gel pH 3.5	30	0.14	1.0	0.3			0.092	1.11

[a] See Figure 5.

TABLE 4: Parameters (Segmental and Global Correlation Times, φ_i, Order Parameter, S_1, and Half-Cone Angle, θ_0) from the Fit of the Independent-Two-Motion Model (eq 2) to the Anisotropy Decay of BSOD in Solution and Immobilized in Sol−Gel Matrices

medium	T (°C)	$\varphi_{segmental}$ (ns)	φ_{global} (ns)	S_1	θ_0
buffer	22	0.3	12	0.82	29
pH 7.4	30	0.2	11	0.83	28
	40	0.3	9	0.79	31
sol−gel	22	0.2	23−30	0.80	31
pH 7.4	30	0.2	24−35	0.80	31
	40	0.2	23−42	0.79	31
sol−gel pH 3.5	30	0.3		0.81	30

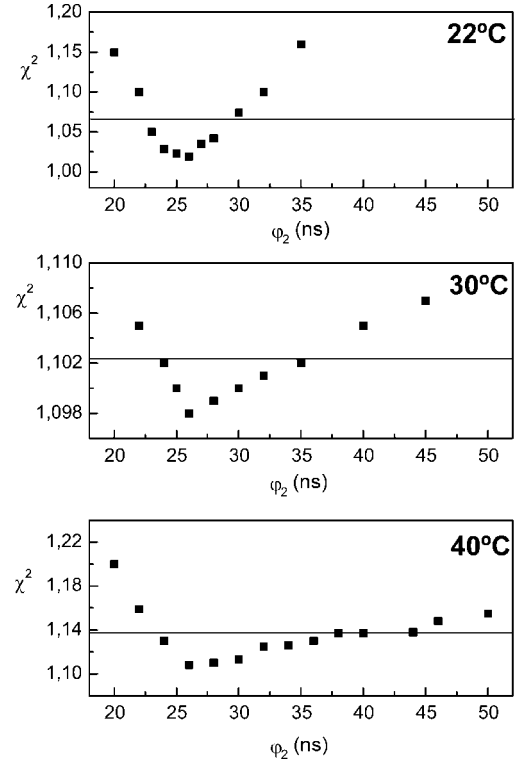

Figure 5. Confidence interval analysis corresponding to one standard deviation (horizontal line) for the rotational correlation time, φ_2, of the entrapped BSOD, recovered at 22, 30, and 40 °C.

altogether with possible fast electronic relaxation processes, as was reported for other peptide/proteins containing single tyrosine.[36] Ultrarapid Förster resonance energy transfer between the two tyrosines of the dimer should be discarded as a depolarization source, since the distance between both residues (∼26 Å) is clearly longer than the characteristic Förster distance for energy transfer between Tyr residues (∼10 Å).[47,48]

For the global motion of BSOD, a value of $\varphi_{global} = 12 \pm 1$ ns was recovered at 22 °C, which is close to the double of that obtained by Ferreira et al.[25] These authors suggested that this correlation time reflected segmental or domain motion of the polypeptide chain containing Tyr-108 and that, given the short lifetime of this residue, fluorescence should be depolarized via these local motions and not from the overall rotation of the protein. However, our results indicate that this global motion is the main motion responsible for the anisotropy decay, which seems consistent with the rigid structure reported for this protein. Since the two subunits of BSOD are strongly bounded through noncovalent interactions, the dimeric BSOD could be modeled with a rigid prolate ellipsoid characterized by an axial ratio $p = 2$. In this case, φ_{global} should be related to the hydrated protein volume V and axial ratio in the following way:[49−52]

$$V = \frac{KT\varphi_{global}}{6\eta}\left(\frac{4}{g_{per}} + \frac{2}{g_{par}}\right) \quad (3)$$

where η is the viscosity of the medium, k is the Boltzman constant, T is the absolute temperature, and g_{per} and g_{par} are rotational Perrin factors depending only on p, which were calculated as[53,54]

$$g_{par} = 2(p^2 - 1)/3p(p - s)$$
$$g_{per} = 2(p^4 - 1)/3p[(2p^2 - 1)s - p] \quad (4)$$
$$s = (p^2 - 1)^{-1/2} \ln[p + (p^2 - 1)^{1/2})]$$

The volume of the equivalent rotating ellipsoid obtained at 22 °C from eqs 3 and 4 is 46 400 ± 4000 Å^3, which is an intermediate value between the volume previously reported from dynamics simulations of the solvated dimeric protein (41 400 Å^3)[55] and that of 51 500 Å^3 calculated taking into account the molecular weight of the dimeric BSOD and a hydratation of 0.3 g of H_2O/g of protein.[25] The temperature variation of φ_{global} provides a further test of the hydrodinamic behavior of the protein. A plot of η/T vs φ_{global} was linear, indicating that the viscosity is the source of the rotational friction and supporting the hypothesis that the dimer rotates as a rigid structure (data not shown).

The anisotropy decay of the entrapped BSOD follows a similar pattern to that observed in solution, i.e., anisotropy tending to zero as time increases (Figure 4). However, the kinetics seems to be slower than in solution. From the fit of eq 1, two rotational correlation times were recovered: a subnanosecond component, similar to the short component observed in solution, and a long second component slower than that obtained for the free protein, whose value shows greater uncertainty, especially at 40 °C (Table 3). This lack of precision in the value of φ_2 was also found for lysozyme[14] and myoglobin[15] entrapped in sol−gel matrices, and was attributed to the short lifetime of the chromophores, which renders the fluorescence decay a little sensitive to long-lived motions. In our case, because the short average fluorescence lifetime of Tyr-108 is ∼1.5 ns, it is difficult to extract precise anisotropy data well beyond 10 lifetimes (∼15 ns). To determine the level of certainty in these correlation times, a confidence interval analysis was performed.[56] Figure 5 illustrates the confidential interval, corresponding to one standard deviation, for the φ_2 values recovered at 22, 30, and 40 °C. A lower limit of ∼26 ns was obtained at 22 °C, with values between 23 and 30 ns consistent with the data. This interval enlarges as temperature increases. For all of these fits, φ_1 was 0.2 ± 0.1 ns and values of β_2 were practically constant, ranging between 0.62 and 0.64. Since for the entrapped BSOD the differences between φ_1 and φ_2 were still higher than those observed in solution, the independent-two-motion model was also considered to interpret the experimental data, and the correlation times φ_1 and φ_2 were directly related to $\varphi_{segmental}$ and φ_{global}, respectively. The latter are shown in Table 4, together with the order parameter S_1 and the corresponding half-cone angle θ_0 calculated from β_2. A value of 31° was obtained for this angle through the three temperatures investigated, which was similar to that determined in solution, indicating that entrapment does not modify the internal dynamics of the protein in the tyrosine region. This result, together with those obtained from the fluorescence spectra, quenching experiments, and fluorescence lifetimes suggests that immobilization does not lead to any major conformational change, at least in the region of protein where the tyrosine residue is located. In consequence, the decrease in the quenching constant of acrylamide, k_Q, observed upon sol−gel entrapment (see Table 2) should probably be associated to a lower rate diffusion of the quencher within the sol−gel pore, as compared to the aqueous solution, and not to a protein conformational change, as had been pointed out before.

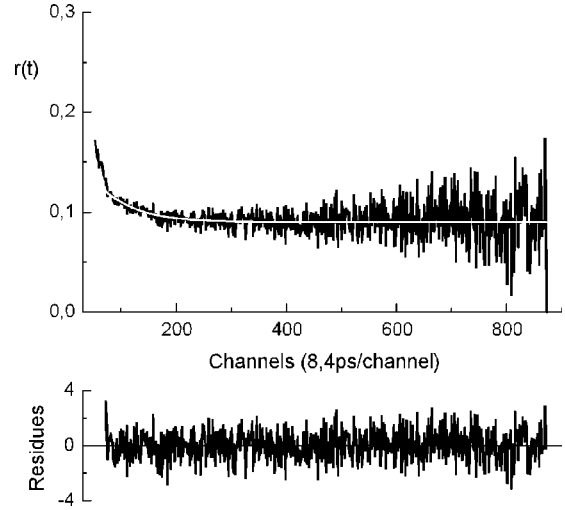

Figure 6. Time-resolved fluorescence anisotropy of BSOD entrapped in a sol−gel matrix upon 48 h of incubation in citrate-phosphate buffer pH 3.5 at 30 °C. The decay fit obtained from eq 1 is superimposed over the collected data. Residuals of the fits are also shown.

Independently of the level of precision in the estimation of φ_{global}, it is clear that the value obtained at 22 °C (where the uncertainty is lower) is approximately 2- to 3-fold longer than that measured in free solution, suggesting certain hindrance in the rotational diffusion of the entrapped BSOD. The isoelectric point of BSOD is about pH 5, and at physiological pH, this protein is therefore negatively charged and likely to be repelled by the silica surface of the sol−gel matrix (negatively charged under the experimental conditions). Consequently, protein−pore electrostatic interactions would not seem to be responsible for this dynamical behavior. With the goal of inducing such interactions and see their effects on the protein global motion, BSOD was encapsulated in a sol−gel matrix which was maintained at pH 3.5 (i.e., below the isoelectric point of the protein) and the photophysical properties and time-resolved fluorescence anisotropy were explored at 30 °C. The decay of the fluorescence emission obtained under these new experimental conditions was best fitted to triexponential functions. Fluorescence fit parameters are shown in Table 1 and are found to be different from those recovered for BSOD in solution and entrapped in sol−gel at pH 7.4. While fluorescent quantum yield and the first and second lifetimes are preserved at low pH, the three relative amplitudes and the longest lifetime are clearly affected, suggesting that, under these new conditions, the environment surrounding Tyr-108 residue is different from that observed at neutral pH. Figure 6 shows the fluorescence anisotropy decay of sol−gel entrapped BSOD at pH 3.5. Comparing the profile of this decay with those observed at pH 7.4 for the free and the encapsulated system (Figure 4), it can be observed that while for these latter the anisotropy tends to zero as time increases, a nonzero residual anisotropy is reached under the acidic conditions at infinite time. The results of the deconvolution analysis of the experimental data are listed in Table 3. From the fit of eq 1, only one correlation time was obtained which was similar to the short component observed in solution and in sol−gel at pH 7.4. The most significant change was the appearance of a residual anisotropy ($r_\infty = 0.092$) instead of the longer correlation time. Following the model previously used, the total anisotropy was interpreted as the product of two

independent depolarizing processes related to the segmental motion of the Tyr residue of the entrapped protein and to the overall rotation of the protein within the matrix pore. The existence of r_∞ can be explained by $\varphi_{global} \rightarrow \infty$ in eq 2 (in this case, $r(t) = r'(t)$ and $r_\infty = r(0)S_1^2$), and therefore, S_1 and the corresponding cone angle θ_0 can be extracted from the r_∞ value (Table 4). These results suggests that, at pH 3.5, the global rotation of the protein is completely hindered, as a consequence of the electrostatic attraction occurring between the pore wall and the protein surface, now positively charged, although the internal dynamics is not altered in comparison with the protein in the bulk solvent and encapsulated at neutral pH.

Taking into account the above results, it is suggested that factors other than electrostatic interactions should be responsible for the dynamical behavior observed for the entrapped BSOD at physiological pH. A 2-fold increase in φ_{global} has been also reported for neutral and anionic small molecules (~0.1 kD) encapsulated in sol−gel matrices[57] and for sol−gel entrapped neutral and negatively charged proteins of 10−16 kD,[16] i.e., having a molecular weight 2−3 times smaller than that of BSOD. The absence of a significant effect of the protein size on its molecular rotation indicates that changes in the effective viscosity of the aqueous solvent surrounding the protein seem to be the main thing responsible for this dynamical behavior (note that changes in the hydrodynamic volume V, due to changes in the size of the solvation shell and/or the occurrence of intermolecular protein aggregation, are unlikely to be promoted by the caging effect on the protein in the sol−gel system).[7] Therefore, the sol−gel encapsulated BSOD exhibits dynamics that are the equivalent of the protein in a solution with a viscosity of around 2−3 cP. This viscosity value is in agreement with that sensed by carbonmonoxy-hemoglobine embedded in silica sol−gel glasses,[58] and slightly lower than that found through NMR (4 cP) and fluorescence (5 cP) experiments.[59,60] Higher viscosity values (~20 cP) have been reported for different solvents confined in sol−gel pores but were attributed to solvent molecules placed on or near the surface of the pores.[61,62] The fact that protein-to-pore size ratio has no measurable effect on the dynamics of the proteins is consistent with templating of the silica matrix around the protein and the production of a constrained layer of surrounding water during gelation.[58] It is known that the effective viscosity of water confined to nanoscopic pores increases with decreasing confinement length.[63] On the basis of this fact, Marassi et al.[58] have, recently, proposed a correlation which allows obtaining a rough approximation of the thickness of the water layer that surrounds the protein in the sol−gel glass from the effective viscosity sensed by the protein. Using this procedure, it is estimated that sol−gel encapsulated BSOD is surrounded by a layer of water that is ~5 nm thick, which indicates that the protein fits in easily within the pore. The existence of this water layer of about 2−3 cP in viscosity is consistent with the value obtained for the quenching constant of acrylamide, k_Q, upon sol−gel entrapment. It is known that the meaning of k_Q can be understood in terms of the frequency of collisions, f_Q, between a fluorophore and a quencher by $k_Q = f_Q k_0$, with k_0 being the diffusion controlled bimolecular rate constant, which may be calculated using the Smoluchowsky equation:[29]

$$k_0 = \frac{4\pi N_A}{10^3}(r_F + r_Q)(D_F + D_Q) \qquad (5)$$

where the factor 4π is the spherical solid angle (indicating that all directions of approach of the spheres lead to reaction), D_F and D_Q are the translation diffusion constants (in cm^2/s), and r_F and r_Q are the hydrodynamic radii (in cm) of fluorophore and quencher, respectively. N_A is Avogadro's number, and the factor 10^3 normalizes the units of k_0 to $M^{-1}\ s^{-1}$. Equation 5 is valid for uncharged spheres and assumes no orientational constraints. Assuming that in solution and in the sol−gel matrix, given the size of the protein, $D_F + D_Q \approx D_Q$ and that the other parameters do not change upon sol−gel entrapment, it is possible to correlate the drop in k_Q with a decrease in D_Q, i.e., $k_Q^{solution}/k_Q^{sol-gel} \approx D_Q^{solution}/D_Q^{sol-gel}$. If the diffusion of acrylamide through the confined water follows, as in solution, the Stokes−Einstein hydrodynamic equation $D_Q = k_B T/(6\pi\eta r_Q)$, then $k_Q^{solution}/k_Q^{sol-gel} \approx \eta^{sol-gel}/\eta^{solution}$ and $\eta^{sol-gel} \approx 1.9 \pm 0.4$ cP, in agreement with the value obtained from φ_{global}.

The above results are also consistent with those reported on the catalytic activity of the sol−gel entrapped BSOD.[22] This activity was found to be fully preserved within the sol−gel matrix, which should be expected considering the thickness of the water layer surrounding the protein. However, the time required for transforming the substrate superoxide radical into hydrogen peroxide was slower than that observed in solution. A slower kinetic response has also been observed for other sol−gel encapsulated enzymes such as horseradish peroxidase, and was attributed to a reduced diffusion of substrates and products through the matrix,[27,64] in agreement with the viscosity values reported in this work, although the negative charge of superoxide radical could also affect its diffusion through the sol−gel matrix.

In conclusion, in this study, we have exploited the intrinsic fluorescence of the enzyme BSOD, coming from its single tyrosine residue, to explore the effects of sol−gel confinement on the protein structural dynamics. Fluorescence spectra, quenching experiments, fluorescence lifetimes, and anisotropy measurements indicate that sol−gel encapsulation does not induce any major conformational change, at least in the region of protein where Tyr residue is located. Regarding the dynamics of the protein, we show that while the segmental rotational properties are not affected by sol−gel encapsulation, its global rotation is clearly affected by the entrapment of the protein, especially below the isoelectric point of BSOD (pI 4.9). Below pI, the overall rotation of the protein is totally arrested, due to the electrostatic attractions between the protein molecule and the negatively charged sol−gel walls. In contrast, above pI, BSOD freely rotates within the matrix pore, albeit 2−3-fold more slowly than in free solution under similar macroscopic solution conditions. These results, together with those obtained from acrylamide quenching experiments indicate that, at neutral pH, BSOD fits in easily within the sol−gel pore, surrounded by a layer of water that is ~5 nm thick and ~2−3 cP in viscosity, which explains that the catalytic activity of the enzyme is fully preserved within the sol−gel matrix.

Acknowledgment. The authors thank the Spanish Ministerio de Educación y Ciencia (MEC) for grants MAT2005-01004, MAT2008-05670, and HP2005-0096 and FCT (Portugal) for research grants. I.P. was partially supported by Instituto de Salud Carlos III. We thank Dr. Alexander Fedorov for his kind help with the time-resolved fluorescence measurements. We are grateful for the useful insights obtained in discussions with Dr. Javier Gómez.

References and Notes

(1) Kandimalla, V. B.; Tripathi, V. S.; Ju, H. *Crit. Rev. Anal. Chem.* **2006**, *36* (2), 73–106.

(2) Rusmini, F.; Zhong, Z.; Feijen, J. *Biomacromolecules* **2007**, *8* (6), 1775–1789.
(3) Peterson, E. S.; Leonard, E. F.; Foulke, J. A.; Oliff, M. C.; Salisbury, R. M.; Kim, D. Y. *Biophys. J.* **2008**, *95*, 322–332.
(4) Simorellis, A. K.; Flynn, P. F. *J. Am. Chem. Soc.* **2006**, *128* (30), 9580–9581.
(5) Sanabria, H.; Kubota, Y.; Waxham, M. N. *Biophys. J.* **2006**, *92* (1), 313–322.
(6) Eggers, D. K.; Valentine, J. S. *J. Mol. Biol.* **2001**, *314*, 911–922.
(7) Eggers, D. K.; Valentine, J. S. *Protein Sci.* **2001**, *10*, 250–2613.
(8) Ellerby, L. M.; Nishida, C. R.; Nishida, F.; Yamanaka, S. A.; Dunn, B.; Valentine, J. S.; Zink, J. I. *Science* **1992**, *255*, 1113–1115.
(9) Gill, I.; Ballesteros, A. *TIBTECH* **2000**, *18*, 282–296.
(10) Jin, W.; Brennan, J. D. *Anal. Chim. Acta* **2002**, *461*, 1–36.
(11) Avnir, D.; Coradin, T.; Lev, O.; Livage, J. *J. Mater. Chem.* **2006**, *16*, 1013–1030.
(12) Martinez-Perez, D.; Ferrer, M. L.; Mateo, C. R. *Anal. Biochem.* **2003**, *322*, 238–242.
(13) Gupta, R.; Chaudbury, N. K. *Biosens. Bioelectron.* **2007**, *22*, 2387–2399.
(14) Pastor, I.; Ferrer, M. L.; Lillo, M. P.; Goìmez, J.; Mateo, C. R. *J. Phys. Chem. B* **2007**, *111* (39), 11603–11610.
(15) Gottfried, D. S.; Kagan, A.; Hoffman, B. M. *J. Phys. Chem. B* **1999**, *103* (14), 2803–2807.
(16) Wheeler, K. E.; Nocek, J. M.; Hoffman, B. M. *J. Am. Chem. Soc.* **2006**, *128* (12), 14782–14783.
(17) Chirico, G.; Cannone, F.; Beretta, S.; Diasproor, A.; Campanini, B.; Bettati, S.; Ruotolo, R.; Mozzarelli, A. *Protein Sci.* **2002**, *11*, 1152–1161.
(18) Sui, X. H.; Cruz-Aguado, J. A.; Chen, Y.; Zhang, Z.; Brook, M. A.; Brennan, J. D. *Chem. Mater.* **2005**, *17*, 1174–1182.
(19) Gonnelli, M.; Strambini, G. B. *Biophys. Chem.* **2003**, *104* (1), 155–169.
(20) Hough, M. A.; Hasnain, S. *Structure* **2003**, *11* (8), 937–946.
(21) Fridovich, I. *Annu. Rev. Biochem.* **1995**, *64*, 97–112.
(22) Pastor, I.; Esquembre, R.; Micol, V.; Mallavia, R.; Mateo, C. R. *Anal. Biochem.* **2004**, *334* (2), 335–343.
(23) Di, J.; Peng, S.; Shen, C.; Gao, Y.; Tu, Y. *Biosens. Bioelectron.* **2007**, *23* (1), 88–94.
(24) Di, J.; Bi, S.; Zhang, M. *Biosens. Bioelectron.* **2004**, *19* (11), 1479–1486.
(25) Ferreira, S. T.; Stella, L.; Gratton, E. *Biophys. J.* **1994**, *66* (4), 1185–1196.
(26) Lyons, T. J.; Nersissian, A.; Goto, J. J.; Zhu, H.; Gralla, E. B.; Valentine, J. S. *J. Biol. Inorg. Chem.* **1998**, *3* (6), 650–662.
(27) Ferrer, M. L.; del Monte, F.; Levy, D. *Chem. Mater.* **2002**, *14*, 3619–3621.
(28) Loura, L. M.; Fedorov, A.; Prieto, M. *Biophys. J.* **1996**, *7*, 1823–1836.
(29) Lakowicz, J. R. *Principles of Fluorescence Spectroscopy*, 2nd ed.; Kluwer Academic/Plenum Press: New York, 1999.
(30) Dale, R. E.; Chen, L. A.; Brand, L. *J. Biol. Chem.* **1977**, *252*, 7500–7510.
(31) Eftink, M. R. *Methods Biochem. Anal.* **1991**, *35*, 127–205.
(32) Sillen, A.; Engelborghs, Y. *Photochem. Photobiol.* **1998**, *67*, 475–486.
(33) Wu, P.; Li, Y. K.; Talalay, P.; Brand, L. *Biochemistry* **1994**, *33*, 7415–7422.
(34) Gryczynski, I.; Steiner, R. F.; Lakowicz, J. R. *Biophys. Chem.* **1991**, *39*, 69–78.
(35) Dietze, E. C.; Wang, R. W.; Lu, A. Y.; Atkins, W. M. *Biochemistry* **1996**, *35*, 6745–6753.
(36) Poveda, J. A.; Prieto, M.; Encinar, J. A.; Gonzaìlez-Ros, J. M.; Mateo, C. R. *Biochemistry* **2003**, *42* (23), 7124–7132.
(37) Noronha, M.; Lima, J. C.; Bastos, M.; Santos, H.; Macąnita, A. L. *Biophys. J.* **2004**, *87*, 2609–2620.
(38) Gauduchon, P.; Wahl, P. H. *Biophys. Chem.* **1978**, *8*, 87–104.
(39) Laws, W. R.; Ross, J. B. A.; Wyssbrod, H. R.; Beechem, J. M.; Brand, L.; Sutherland, J. C. *Biochemistry* **1986**, *25*, 599–607.
(40) Lux, B.; Gérard, D.; Laustriat, G. *FEBS Lett.* **1977**, *80*, 66–70.
(41) Unruh, J. R.; Liyanage, M. R.; Johnson, C. K. *J. Phys. Chem. B* **2007**, *111* (19), 5494–5502.
(42) Soengas, M. S.; Mateo, C. R.; Salas, M.; Acunã, A. U.; Gutieìrrez, C. *J. Biol. Chem.* **1997**, *272* (1), 295–302.
(43) Zheng, L. L.; Reid, W. R.; Brennan, J. D. *Anal. Chem.* **1997**, *69* (19), 3940–3949.
(44) Jähnig, F. *Proc. Natl. Acad. Sci. U.S.A.* **1979**, *76*, 6361–6365.
(45) Lipari, G.; Szabo, A. *Biophys. J.* **1980**, *30*, 489–506.
(46) Kinosita, K.; Kawato, S.; Ikegami, A. *Biophys. J.* **1977**, *20*, 289–305.
(47) Ross J. B. A.; Laws W. R.; Rousslang K. W.; Wyssbrod H. R. In *Topics in fluorescence spectroscopy*; Lakowicz, J. R., Ed.; Plenum Press: New York, 1992; Vol. 3, pp 1−63.
(48) Saito, Y.; Tachibana, H.; Hayashi, H.; Wada, A. *Photochem. Photobiol.* **1981**, *33*, 289–295.
(49) Wahl, P. H. In *Time-resolved Fluorescence Spectroscopy in Biochemistry and Biology*; Cundall, R. B.; Dale, R. E., Eds.; Nato Asci Series A, Vol. 69; Plenum Press: New York, 1983.
(50) Montejo, J. M.; Navqvi, K. R.; Lillo, M. P.; González, J.; Acuña, A. U. *Biochemistry* **1992**, *31*, 7580–7586.
(51) Soengas, M. S.; Mateo, C. R.; Salas, M.; Acunã, A. U.; Gutiérrez, C. *J. Biol. Chem.* **1997**, *272* (1), 303–310.
(52) Steel, C.; Naqvi, R. K. *J. Phys. Chem.* **1995**, *95*, 10713–10718.
(53) Perrin, F. *J. Phys. Radium* **1936**, *7*, 1–11.
(54) Cantor, C. R.; Shimmel, P. R. *Biophysical Chemistry, Part II*; Freeman W.H. and Co.: San Francisco, CA, 1980.
(55) Falconi, M.; Melchionna, S.; Desideri, A. *Biophys. Chem.* **1999**, *81* (3), 197–205.
(56) Beechem, J. M.; Gratton, E.; Ameloot, M.; Knutson, J. R.; Brand, L. In *Topics in Fluorescence Spectroscopy*; Lakowicz, J. R., Ed.; Plenum Press: New York, 1991; Vol. 2, pp 241−305.
(57) Wheeler, K. E.; Lees, N. S.; Gurbiel, R. J.; Hatch, S. L.; Nocek, J. M.; Hoffman, B. M. *J. Am. Chem. Soc.* **2004**, *126*, 13459–13463.
(58) Massari, A. M.; Finkelstein, I. J.; Fayer, M. D. *J. Am. Chem. Soc.* **2005**, *128*, 3990–3997.
(59) Winter, R.; Hua, D. W.; Sing, X.; Mantulin, W.; Jonas, J. *J. Phys. Chem.* **1990**, *94*, 2706–2713.
(60) Ferrer, M. L.; del Monte, F.; Levy, D. *J. Phys. Chem. B* **2001**, *105*, 11076–11080.
(61) Loughnane, B. J.; Farrer, R. A.; Scodinu, A.; Fourkas, J. T. *J. Chem. Phys.* **1999**, *111*, 5116–5122.
(62) Loughnane, B. J.; Farrer, R. A.; Scodinu, A.; Reilly, T.; Fourkas, J. T. *J. Phys. Chem. B* **2000**, *104*, 5421–5429.
(63) Tan, H. S.; Piletic, I. R.; Fayer, M. D. *J. Chem. Phys.* **2005**, *122*, 174501.
(64) Bathia, R. B.; Brinker, J. *Chem. Mater.* **2000**, *12*, 2434–2441.

JP805368S